AAC
Journals.ASM.org

Structural Insights into and Activity Analysis of the Antimicrobial Peptide Myxinidin

Marco Cantisani,[a,b,c] Emiliana Finamore,[d] Eleonora Mignogna,[d] Annarita Falanga,[a,b] Giovanni Francesco Nicoletti,[e] Carlo Pedone,[a,b] Giancarlo Morelli,[a,b] Marilisa Leone,[b] Massimiliano Galdiero,[d] Stefania Galdiero[a,b]

Department of Pharmacy, CIRPEB, and DFM, University of Naples Federico II, Naples, Italy[a]; Istituto di Biostrutture e Bioimmagini, CNR, Naples, Italy[b]; Center for Advanced Materials for Healthcare IIT@CRIB, Istituto Italiano di Tecnologia, Naples, Italy[c]; Department of Experimental Medicine, II University of Naples, Naples, Italy[d]; Dipartimento Multidisciplinare di Specialità Medico-Chirurgiche e Odontoiatriche, II University of Naples, Naples, Italy[e]

The marine environment has been poorly explored in terms of potential new molecules possessing antibacterial activity. Antimicrobial peptides (AMPs) offer a new potential class of pharmaceuticals; however, further optimization is needed if AMPs are to find broad use as antibiotics. We focused our studies on a peptide derived from the epidermal mucus of hagfish (*Myxine glutinosa* L.), which was previously characterized and showed high antimicrobial activity against human and fish pathogens. In the present work, the activities of myxinidin peptide analogues were analyzed with the aim of widening the original spectrum of action of myxinidin by suitable changes in the peptide primary structure. The analysis of key residues by alanine scanning allowed for the design of novel peptides with increased activity. We identified the amino acids that are of the utmost importance for the observed antimicrobial activities against a set of pathogens comprising both Gram-negative and Gram-positive bacteria. Overall, optimized bactericidal potency was achieved by adding a tryptophan residue at the N terminus and by the simultaneous substitution of residues present in positions 3, 4, and 11 with arginine. These results indicate that the myxinidin analogues emerge as an attractive alternative for treating drug-resistant infectious diseases and provide key insights into a rational design for novel agents against these pathogens.

The rise in antibiotic resistance among pathogenic bacteria and the declining rate of novel drug discovery have become major threats to global health care, driving research into the investigation of new antibacterial classes and novel drugs in order to defend against infectious diseases, especially those caused by multidrug-resistant (MDR) organisms (1, 2). Antimicrobial peptides (AMPs), being an essential part of the innate immune response, with both direct microbicidal and pleiotropic immunomodulatory properties (3, 4), are promising candidates as future therapeutics. AMPs have been isolated and characterized from tissues and organisms representing virtually every kingdom and phylum ranging from prokaryotes to humans; thus, they are ancient host defense effector molecules present in organisms across the evolutionary spectrum (5). Although AMPs have been isolated from such an array of divergent organisms (e.g., microorganisms, insects, invertebrates, amphibians, plants, birds, and mammals) (6, 7), most share biophysical features that appear to be essential for antimicrobial efficacy (8). Since their discovery >30 years ago, several hundred AMPs have been described (for databases, see references 5, 9, and 10). The majority of characterized AMPs are small sequences, comprised of 12 to 60 amino acids with molecular masses of <10 kDa; most of them fall into one of two main structural groups, linear/α-helical or disulfide stabilized/β-sheet. The majority of remaining peptides can be classified as extended helices and cyclized loops. Most AMPs display similar modes of action against a wide range of microbes, sharing several common properties, and they tend to display broad-spectrum antimicrobial activity and a cationic charge at physiological pH.

The marine environment is poorly explored in terms of potential pharmaceuticals. It contains a tremendous organism diversity, which might be a good source of novel AMPs. AMPs have been identified in fish epidermal mucus, which also contains lysozyme, proteases, and lectins (11). The mucus stratus secreted by goblet or mucus cells in fish epidermis functions as a physical and biochemical barrier between fish and their aquatic environment. Fish live in a microbe-rich environment and are easily vulnerable to invasion by pathogenic or opportunistic microbes. The mucus layer provides mechanical protective functions, but the prevention of colonization by parasites, bacteria, and fungi is also complemented by the molecules present in the mucus having antimicrobial characteristics. Thus, fish are a good source of AMPs, including defensins, cathelicidins, hepcidins, histone-derived peptides, and piscidins (12, 13).

One of the most recent cationic AMPs discovered in fish mucus is the peptide myxinidin, identified from the epidermal mucus of hagfish (*Myxine glutinosa* L.) by Subramanian, Ross, and MacKinnon (14). Myxinidin is a 12-amino-acid peptide with a molecular mass of 1,327 Da and with the following amino acid sequence from the N terminus: Gly-Ile-His-Asp-Ile-Leu-Lys-Tyr-Gly-Lys-Pro-Ser (14). Myxinidin has shown activity against a broad range of bacteria and yeast pathogens at a minimum bactericidal concentration (MBC) in the micromolar range, and it represents one of the shortest natural AMPs discovered so far. The useful characteristic of the bioactivity of myxinidin is its ability to

Received 14 February 2014 Returned for modification 13 March 2014
Accepted 16 June 2014
Published ahead of print 23 June 2014
Address correspondence to Massimiliano Galdiero, massimiliano.galdiero@unina2.it, or Stefania Galdiero, stefania.galdiero@unina.it.
Supplemental material for this article may be found at http://dx.doi.org/10.1128/AAC.02395-14.

doi:10.1128/AAC.02395-14

function in the presence of high salt concentrations and the absence of hemolytic activity against mammalian red blood cells, making it a suitable candidate for combating human infectious pathogens (14, 15).

Since the rational design of AMPs represents a straightforward approach to obtaining a peptide with better therapeutic characteristics, an analysis of the structural elements responsible for the antimicrobial action of myxinidin was initiated (16). Here, to address the influence of each amino acid residue of myxinidin on its antimicrobial activity, an alanine scanning analysis was carried out, together with the synthesis of novel analogues. Alanine scanning has commonly been used to probe peptides, because the convenient substitution of a residue side chain by a methyl group provides an effective tool for assessing the side chain responsible for activity (17). Besides getting better insights into the structure-function relationship of the peptide, the results have provided important information for the further modification of key residues for the optimization of myxinidin-based anti-infective agents and the design of myxinidin analogues to be employed in biophysical studies for analyzing the membranotropic behavior of myxinidin and its putative mechanism of action.

MATERIALS AND METHODS

Materials. The amino acids used for the peptide synthesis, the Rink amide 4-methylbenzhydrylamine (MBHA) resin, and the activators *N*-hydroxybenzotriazole (HOBT) and *O*-benzotriazole-*N*,*N*,*N*′,*N*′-tetramethyl-uronium-hexafluorophosphate (HBTU) were purchased from Novabiochem (Gibbstown, NJ, USA). Acetonitrile (ACN) was from Reidel-deHaën (Seelze, Germany) and *N*,*N*-dimethylformamide (DMF) from LabScan (Dublin, Ireland). All other reagents were from Sigma-Aldrich (Milan, Italy). Liquid chromatography-mass spectrometry (LC-MS) analyses were performed on an LC-MS Thermo Finnigan with an electrospray source (MSQ) on a Phenomenex Jupiter 5-μm C_{18} 300-Å (150 by 4.6 mm) column. Purification was carried out on a Phenomenex Jupiter 10-μm Proteo 90-Å (250 by 10 mm) column. Lipopolysaccharide (LPS) of *Escherichia coli* O111:B4 was purchased from Sigma-Aldrich. Mueller-Hinton broth (MHB) and Mueller-Hinton agar (MHA) were purchased from Oxoid (Basingstoke, Hampshire, United Kingdom), and cation-adjusted Mueller-Hinton II broth (212322) was purchased from BD (Franklin Lakes, NJ, USA).

Peptide synthesis. Peptides were synthesized using a standard solid-phase-9-fluorenylmethoxycarbonyl (Fmoc) method, as previously reported (18). Briefly, 50 μmol of peptides was synthesized on a Rink amide resin (0.54 mmol/g) (for C-terminal NH_2 peptides) or on a Wang resin (0.9 mmol/g) (for C-terminal COOH peptides) by consecutive deprotection, coupling, and capping cycles; deprotection involved 30% piperidine in DMF for 5 min (2×), coupling involved 4 equivalents of amino acid plus 4 equivalents of HBTU/HOBT (0.45/0.50 M in DMF) for 25 min, and capping involved acetic anhydride/DIPEA/DMF, 15/15/70 (vol/vol/vol), for 5 min (DIPEA, *N*,*N*-diisopropylethylamine). The peptides were cleaved from the resin and deprotected by treatment with trifluoroacetic acid (TFA) and precipitated in cold ethyl ether. Analysis of the crude peptides was performed by electrospray ionization (ESI) LC-MS (Thermo Electron Finnigan Surveyor MSQ single quadrupole) using a gradient of acetonitrile (0.1% TFA) in water (0.1% TFA) from 5 to 60% in 20 min and a Jupiter column (4 μm, Proteo 90 Å, 50 by 2.0 mm). The peptides were purified by preparative reverse-phase high-performance liquid chromatography (RP-HPLC) (Shimadzu SPD-10A VP UV-Vis detector) using a gradient of acetonitrile (0.1% TFA) in water (0.1% TFA) from 5 to 60% in 15 min and a Jupiter column (10 μm, Proteo 90 Å, AXIA packed, 250 by 21.20 mm). All purified peptides were obtained with good yields (70 to 80%). Tables 1 and 2 show the sequences of all the synthesized peptides.

TABLE 1 Myxinidin analogue comparison with respect to charge, pI, μHrel, and percent helicity

Peptide	Sequence[a]	Charge	pI[b]	μHrel[c]	% helicity in TFE
Myxinidin	H_2N-GIHDILKYGKPS-$CONH_2$	+2	8.31	0.44	63
G 1	H_2N-**A**IHDILKYGKPS-$CONH_2$	+2	8.55	0.45	64
I 2	H_2N-G**A**HDILKYGKPS-$CONH_2$	+2	8.51	0.33	62
H 3	H_2N-GI**A**DILKYGKPS-$CONH_2$	+2	8.5	0.43	63
D 4	H_2N-GIH**A**ILKYGKPS-$CONH_2$	+2	9.7	0.38	65
I 5	H_2N-GIHD**A**LKYGKPS-$CONH_2$	+2	8.51	0.35	67
L 6	H_2N-GIHDI**A**KYGKPS-$CONH_2$	+2	8.51	0.4	68
K 7	H_2N-GIHDIL**A**YGKPS-$CONH_2$	0	6.74	0.33	69
Y 8	H_2N-GIHDILK**A**GKPS-$CONH_2$	+2	8.6	0.45	63
G 9	H_2N-GIHDILKY**A**KPS-$CONH_2$	+2	8.5	0.46	62
K 10	H_2N-GIHDILKYG**A**PS-$CONH_2$	0	6.74	0.43	59
P 11	H_2N-GIHDILKYGK**A**S-$CONH_2$	+2	8.51	0.46	64
S 12	H_2N-GIHDILKYGKP**A**-$CONH_2$	+2	8.51	0.47	66

[a] Amino acid substitutions are indicated in bold.
[b] The pI was calculated with the program ProtParam.
[c] The relative hydrophobic moment (μHrel) of a peptide is its hydrophobic moment relative to that of a perfectly amphipathic peptide. This gives a better idea of the amphipathicity using different scales. Thus, a value of 0.5 indicates that the peptide has about 50% of the maximum possible amphipathicity. The program HydroMCalc that was used to obtain these hydrophobicity data does not differentiate between amidated and free COOH.

The peptide content for all experiments was determined by UV spectroscopy by constructing a Beer-Lambert reference line for each peptide.

CD measurements. Circular dichroism (CD) spectra were recorded using a Jasco J-715 spectropolarimeter in a 0.1-cm quartz cell at room temperature. The spectra are an average of 3 consecutive scans from 250 to 195 nm, recorded with a bandwidth of 3 nm, a time constant of 16 s, and a scan rate of 10 nm/min. The spectra were recorded and corrected for the blank sample. The mean residue ellipticities (MRE) were calculated using the equation MRE = *Obsd*/(*lcn*), where *Obsd* is the ellipticity measured in millidegrees, *l* is the path length of the cell in cm, *c* is the peptide concentration in mol/liter, and *n* is the number of amino acid residues in the peptide. All measurements were made in 5 mM phosphate buffer (pH 7.5), using peptide concentrations of 100 μM, at different percentages of trifluoroethanol (TFE)-to-phosphate buffer (Fig. 1 and Table 1) and in dioleylphosphatidylethanolamine (DOPE)-to-dioleylphosphatidylglycerol (DOPG) 4:1 small unilamellar vesicles (SUVs) at a peptide-to-lipid ratio of 0.5 mol/mol. The percentage of helical content was calculated from measurements of helical mean residue ellipticity at 222 nm (19, 20). We used θ_{222} values of 0 and −40,000 $(1 - 2.5/n)$ degrees · cm^2 $dmol^{-1}$ per amino acid residue for 0% and 100% helicity, respectively, where *n* is the number of amino acid residues.

NMR analysis. Nuclear magnetic resonance (NMR) spectra were recorded at 298 K on a Varian Unity INOVA 600 spectrometer, equipped with a cold probe, and a Varian Unity INOVA 400 spectrometer provided with *z* axis pulsed-field gradients and a triple resonance probe.

The NMR samples consisted of peptide (1 mg) dissolved in either 600 μl of a 10 mM sodium phosphate buffer solution (pH 7.4), with 10% (vol/vol) D_2O (99.8% d; Armar Scientific, Switzerland) or a mixture of 10 mM sodium phosphate buffer (pH 7.4)-TFE (2-2-2 trifluorethanol-d_3, 98% d; Armar Chemicals, Switzerland) (50/50 [vol/vol]).

Water suppression was achieved with the double pulsed-field gradient selective echo (DPFGSE) sequence (21). One-dimensional (1D) [^{1}H] proton experiments were recorded with a relaxation delay d1 of 1.5 s and 64 scans. Proton resonances (see Table S1 in the supplemental material) were assigned with a canonical protocol (22) relying on a comparison of two-dimensional (2D) [^{1}H, ^{1}H] total correlation spectroscopy (TOCSY) (23) (1,024 × 128 total data points, 16 scans per t1 increment, 70-ms mixing

TABLE 2 Myxinidin analogue comparison with respect to charge, pI, μHrel, and percent helicity

Peptide	Sequence[a]	Charge	pI[b]	μHrel[c]	% helicity in TFE
Myxinidin[d]	H_2N-GIHDILKYGKPS-$CONH_2$	+2	8.31	0.44	63
WMR[d]	H_2N-**W**GI**RR**ILKYGK**R**S-$CONH_2$	+6	11.73	0.46	62
WMR-COOH	H_2N-**W**GI**RR**ILKYGK**R**S-COOH	+5	11.73	0.46	60
MH3R[d]	H_2N-GI**R**DILKYGKPS-$CONH_2$	+3	9.7	0.49	61
WMH3R	H_2N-**W**GI**R**DILKYGKPS-$CONH_2$	+3	9.7	0.34	62
WMH3R-COOH	H_2N-**W**GI**R**DILKYGKPS-COOH	+2	9.7	0.34	60
MD4R[d]	H_2N-GIH**R**ILKYGKPS-$CONH_2$	+4	10.29	0.46	64
WMD4R	H_2N-**W**GIH**R**ILKYGKPS-CONH2	+4	10.29	0.30	60
WMD4R-COOH	H_2N-**W**GIH**R**ILKYGKPS-COOH	+3	10.29	0.30	58

[a] Amino acid substitutions are indicated in bold.
[b] The pI was calculated with the program ProtParam.
[c] The relative hydrophobic moment (μHrel) of a peptide is its hydrophobic moment relative to that of a perfectly amphipathic peptide. This gives a better idea of the amphipathicity using different scales. A value of 0.5 thus indicates that the peptide has about 50% of the maximum possible amphipathicity. The program HydroMCalc that was used to obtain these hydrophobicity data does not differentiate between amidated and free COOH.
[d] The data relative to these peptides were obtained in a previous work (16).

time) and nuclear Overhauser enhancement spectroscopy (NOESY) (24) (2,048 × 256 total data points, 64 scans per t1 increment, 200- and 300-ms mixing times). Side chain assignments were confirmed by analysis of the 2D [^{1}H, ^{1}H] double quantum filter correlation spectroscopy (DQFCOSY) (25) spectrum (2,048 × 256 total data points, 64 scans per t1 increment). Chemical shifts were referenced to 3-(trimethylsilyl)propionic-2,2,3,3-d_4 acid sodium salt (TSP) (99% d; Armar Scientific, Switzerland).

The Varian software VNMRJ 1.1D (Varian by Agilent Technologies,

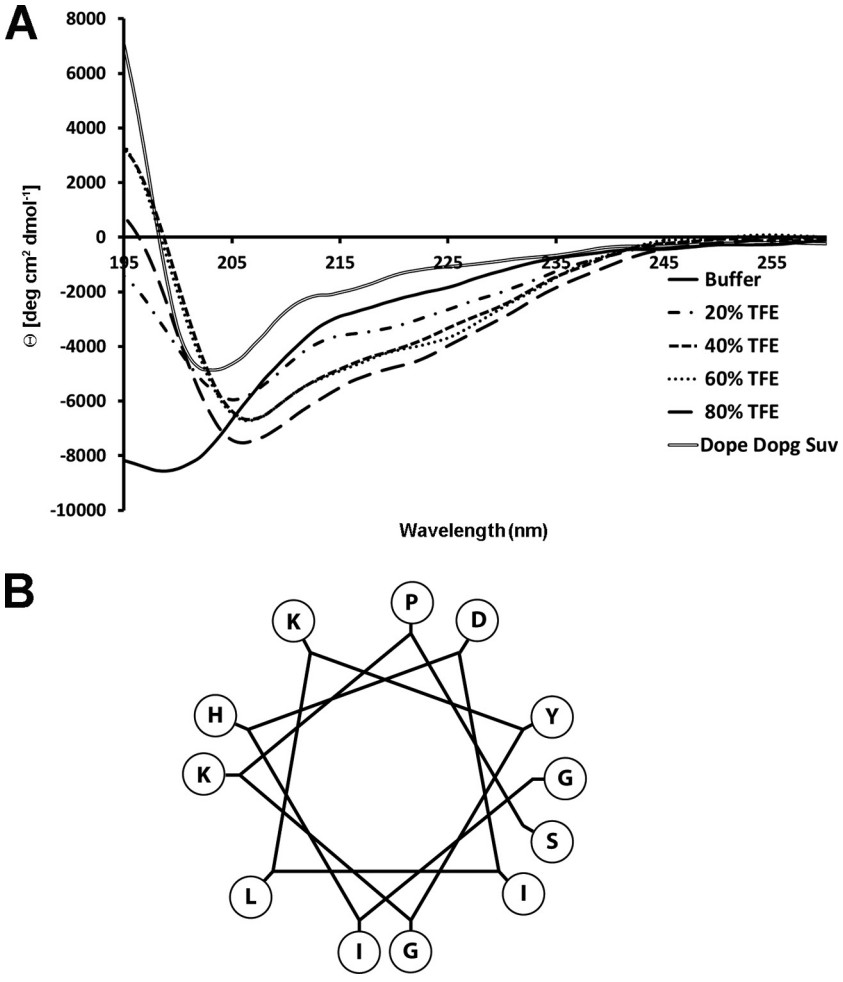

FIG 1 (A) Circular dichroism spectra of the native myxinidin peptide in buffer, different percentages of TFE, and DOPE/DOPG SUVs. (B) Helical wheel representation showing the amphipathicity of the peptide.

Italy) was used for NMR data processing and analysis of the 1D experiments. The program NEASY (26) (http://www.nmr.ch/) was implemented for analysis of the 2D NMR spectra.

The myxinidin solution structure was calculated with the program CYANA (version 2.1) (27). Distance constraints were generated from the 2D NOESY 200 experiment. Angular constraints were obtained with the Grid Search module of CYANA. Calculations started from 100 random conformers; in the end, 20 structures (i.e., the ones with the lowest CYANA target functions) were considered representative, included in the NMR ensemble, and further analyzed with MOLMOL (28) and iCing (https://nmr.le.ac.uk/) (29, 30).

Microorganisms. The strains used for the antimicrobial assays were Gram-negative *E. coli* strain ATCC 11219, *Pseudomonas aeruginosa* strain ATCC 13388, *Salmonella enterica* subsp. *enterica* serovar Typhimurium strain ATCC 14028, *Klebsiella pneumoniae* ATCC 10031, and Gram-positive *Staphylococcus aureus* strain ATCC 6538.

To standardize the bacterial cell suspension for the antibacterial activity assay, fresh colonies of each strain cultured on MHA plates were used to inoculate MHB medium and grown overnight. Hundred-fold dilutions of the bacterial suspension were then resuspended in fresh medium and further incubated at 37°C until there was visible turbidity. This log-phase inoculum was resuspended in 0.9% sterile saline to reach an appropriate optical density at 600 nm (OD_{600}) value (with a Bio-Rad microplate reader; Bio-Rad Laboratories, Hercules, CA) corresponding to a concentration of about 1×10^8 CFU/ml. This standardized inoculum was diluted 1:10 in MHB, and the inoculum size was confirmed by colony counting.

Antimicrobial activity assays. Susceptibility testing was performed using the broth microdilution method outlined by the Clinical and Laboratory Standards Institute using sterile 96-well microtiter plates (Falcon, Franklin Lakes, NJ). Serial 2-fold dilutions (0.1 to 50 μM) of each peptide were prepared in cation-adjusted Mueller-Hinton broth (CAMHB) at a volume of 100 μl/well. Each well was inoculated with 5 μl of the standardized bacterial inoculum, corresponding to a final test concentration of about 5×10^5 CFU/ml. The antimicrobial activities were expressed as the MIC, the lowest concentration of peptide at which 100% inhibition of microbial growth was observed after 24 h of incubation at 37°C. When a statistical difference was observed, we performed a further set of triplicate antibacterial experiments using peptides at concentrations close to the average MIC obtained.

All experiments were performed in triplicate, and the means ± standard deviations are reported.

Eukaryotic cell cytotoxicity. Vero cells were exposed to increasing concentrations of compounds, and the number of viable cells was determined using the 3-(4,5-dimethylthiazol-2-yl)-2,5-diphenyltetrazolium bromide (MTT) assay that is based on the reduction of the yellowish MTT to the insoluble and dark blue formazan by viable and metabolically active cells (31). Vero cells were subcultured in 96-well plates at a seeding density of 2×10^4 cells/well and treated with peptides at concentrations ranging from 1 to 200 μM for 3, 10, and 24 h. The medium was then gently aspirated, MTT solution (5 mg/ml) was added to each well, and the cells were incubated for a further 3 h at 37°C. The medium with MTT solution was removed, and the formazan crystals were dissolved with dimethyl sulfoxide. The absorption values at 570 nm were measured using a Bio-Rad microplate reader. The viability of Vero cells in each well was presented as a percentage of control cells. All experiments were performed in triplicate, and the means ± standard deviations are reported.

Hemolytic assay. The hemolytic activities of the peptides were determined using fresh human erythrocytes from healthy donors. The blood was centrifuged, and the erythrocytes were washed three times with 0.9% NaCl. Peptides were added to the erythrocyte suspension (5% [vol/vol]), at a final concentration ranging from 1 to 200 μM in a final volume of 100 μl. The samples were incubated with agitation at 37°C for 60 min. The release of hemoglobin was monitored by measuring the absorbance (Abs) of the supernatant at 540 nm. The control for zero hemolysis (blank) consisted of erythrocytes suspended in the presence of peptide solvent. Hypotonically lysed erythrocytes were used as a standard for 100% hemolysis. The percentage of hemolysis was calculated using the equation % hemolysis = $[(Abs_{sample} - Abs_{blank})/(Abs_{total\ lysis} - Abs_{blank})] \times 100$. All experiments were performed in triplicate, and the standard deviations are reported.

RESULTS

Peptide design and synthesis. In order to evaluate the role of each amino acid side chain on the peptide activity, a complete Ala scanning of myxinidin was executed. Alanine peptides were designed, substituting all position-native residues with alanine (Table 1). Their antimicrobial activities were tested against Gram-positive (*S. aureus*) and Gram-negative (*E. coli*, *P. aeruginosa*, *S.* Typhimurium, and *Klebsiella pneumoniae*) bacteria. In order to determine the analogue with the highest activity, several other sequences were designed, and their sequences are reported in Table 2. In particular, the most active peptides were also synthesized with the free C terminus (COOH) in order to understand the role of capping at the C terminus.

All peptides were obtained with a good (>70%) yield of the purified compounds and with a purity of >98% (see Fig. S1 in the supplemental material for examples of LC-MS). Their sequences are reported in Tables 1 and 2, together with the isoelectric point, the relative hydrophobic moment (μHrel), and the percentage of helicity in TFE.

Circular dichroism. Analysis of the secondary structure of the peptides was carried out by CD in phosphate buffer, 60% TFE, and DOPE-to-DOPG 4:1 SUVs to mimic the hydrophobic environment of the membrane. The DOPE-to-DOPG composition of SUVs was chosen because it is widely used to mimic the membrane bilayer of Gram-negative bacteria and in particular of *E. coli* (32). All the peptides showed a negligible secondary structure in buffer, with a deep minimum at 200 nm and a shallow minimum at 224 nm. A helical structure was induced by the nonpolar environment of TFE, a mimic of hydrophobicity, and an α-helical inducer. In buffer, the peptides do not assume a defined conformation, while in the membrane-mimicking environment, they seem to approach a helix-like conformation. In particular, all the peptide analogues in TFE and in SUVs showed a typical α-helix spectrum, with a double minimum at 208 nm and a shoulder at 220 nm. The percentage of helical content was calculated from measurements of helical mean residue ellipticity at 222 nm (19). We used θ_{222} values of 0 and −40,000 $(1 - 2.5/n)$ degrees $cm^2 \cdot dmol^{-1}$ per amino acid residue for 0% and 100% helicity, respectively, where n is the number of amino acid residues. The percentages of helicity in TFE of the various mutant peptides are reported in Table 1, and the CD spectra of the native myxinidin sequence are reported in Fig. 1A. All the analogues retained approximately a helicity similar to that of myxinidin (0 to ≤6% helical content difference).

NMR studies. NMR studies of myxinidin were first carried out in sodium phosphate buffer (10 mM [pH 7.4]). Under these experimental conditions, the peptide is flexible and lacks ordered secondary structure elements, as clearly indicated by the almost complete absence of NOE cross-peaks in the 2D [^{1}H, ^{1}H] NOESY 300 experiment (see Fig. S2A in the supplemental material) and by the poor signal dispersion in the 1D spectrum (see Fig. S3B in the supplemental material).

In contrast, it was possible to achieve a complete peptide struc-

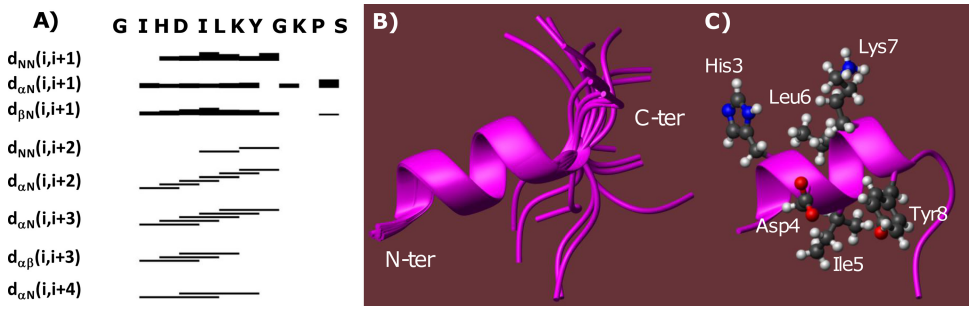

FIG 2 (A) NOE intensity pattern. The myxinidin amino acid sequence is given at the top. Sequential and medium-range NOEs are represented by bars connecting different residues; the thickness of the lines reflects the corresponding NOE intensities. NOE connectivities involving the H_N, Hα, and Hβ of residue i and amide protons of residue i + x are represented by $d_{NN}(i,i + x)$, $d_{\alpha N}(i,i + x)$, and $d_{\beta N}(i,i + x)$, respectively, whereas $d_{\alpha\beta}(i,i + 3)$ denotes a NOE cross-peak between the Hα and Hβ protons of the i and i + 3 residues, respectively. (B) Overlay on the backbone atoms (residues 2 to 9) of 20 myxinidin NMR conformers. N-ter, N terminus; C-ter, C terminus. (C) Ribbon representation of the best CYANA structure (i.e., the one with the lowest target function: n.1); 142 distance constraints (54 intraresidue, 62 short-, and 26 medium-range) and 42 angle constraints were incorporated in the final structure calculation.

ture characterization in a mixture of sodium phosphate-TFE (50/50 [vol/vol]) (see Fig. S3 in the supplemental material). TFE is a useful structuring cosolvent to investigate the inherent conformational preferences of proteins and peptides (33).

Chemical shift deviations from random coil values for Hα protons (34) show the tendency of myxinidin to assume helical secondary structure elements in the region from His^3 to Lys^7 (see negative deviations in the diagram of Fig. S4 in the supplemental material). The NOE pattern, including many contacts like H_Ni-H_N(i + 1), H_Ni-H_N(i + 2), H_αi-H_N(i + 2), H_αi-H_N(i + 3), H_αi-H_β(i + 3), and H_αi-H_N(i + 4), confirms the presence of an ordered helical segment in the peptide (Fig. 2A).

Moreover, the NOE connectivities Hα10-Hδδ'11 indicate that Pro_{11} is in *trans*-configuration (22).

Three-dimensional peptide models were built with the software CYANA (see Table S2 in the supplemental material) (18). NMR structures (Fig. 2B and C) obey the experimental constraints well, as indicated by the low value of the CYANA target function (see Table S2). The structures are well defined in the region encompassing residues Ile_2-Gly_9 (see low root mean square deviation [RMSD] values in Table S2). Analysis with the program MOLMOL (28) indicates the presence of an alpha helix between Ile^2 and Tyr^8, whereas the last few C-terminal residues (Gly^9, Lys^{10}, Pro^{11}, and Ser^{12}) do not participate in any ordered secondary structure elements.

In summary, in the presence of TFE the peptide assumes an ordered α-helical structure, covering >50% of the sequence (7/12 amino acids), as supported by CD data.

Toxicity. To confirm that myxinidin and its alanine scanning analogues do not exert toxic effects on cells, monolayers of Vero cells were exposed to different concentrations (1 to 200 μM) of each compound for 3, 10, and 24 h, and cell viability was quantified by the MTT assay. No statistical difference was observed between the viability of the control (untreated) cells and that of cells exposed to the peptides (Fig. 3A and C) up to the concentration used in antimicrobial testing. Minimal toxicity was observed only at concentrations that were considerably higher than those required for antimicrobial activity.

Antibacterial activity. In order to assess the role of each individual amino acid in the antimicrobial activity of myxinidin, we performed an alanine scanning study by systematically replacing single residues with the neutral amino acid Ala (Fig. 4 and 5A). The antimicrobial activities of these analogues were analyzed by the broth microdilution method against the Gram-negative bacteria (*E. coli*, *P. aeruginosa*, *S.* Typhimurium, *K. pneumoniae*) (Fig. 4) and a Gram-positive bacterium (*S. aureus*) (Fig. 5A). The results are shown in Table S3 in the supplemental material.

The structural data showed that all myxinidin analogues conserved similar α-helical structures; therefore, the identity and character of the amino acids in the peptide are of primary importance for their activity. In fact, the data pointed out that the following substitutions had marked impact on the antimicrobial activity of the natural peptide on Gram-negative bacteria, exhibiting much higher MIC values than those of myxinidin, against all microorganisms. These substitutions were (i) the replacement of the hydrophobic Ile^2 and Leu^6 (peptides I2 and L6, respectively), (ii) the change of the negatively charged residue Asp^4 (peptide D4), (iii) the substitution of the aromatic residue Tyr_8 (peptide Y8), and (iv) the replacement of the C-terminal polar residue Ser^{12} (peptide S12). In contrast, substitution with Ala of the amino acids present in all the other positions (G1, Gly to Ala; H3, His to Ala; I5, Ile to Ala; G9, Gly to Ala; and P11, Pro to Ala) preserved the antibacterial activity of the parent peptide on some bacteria and increased its activity against others.

The replacement of Ile^2 and Leu^6 markedly reduced the antibacterial activity, indicating that in those positions is preferred a hydrophobic residue with a branched chain; it can be hypothesized that these residues help the insertion of the peptide into the hydrophobic core of the membrane, and this view is supported by the fact that they are both localized on the hydrophobic face of the helical wheel (Fig. 1B).

The change of the negatively charged residue Asp^4 (on the polar face of the helix) reduces activity because this position has to be occupied by a charged residue. The substitution of Ser^{12} with Ala significantly impairs the activity of the native peptide, indicating that a polar residue on the hydrophobic face of the peptide is fundamental for activity. This was a key feature also of other AMPs, as previously reported (35, 36).

The substitution of the aromatic Tyr^8 determines a decrease in the activity in all bacteria. Aromatic residues are rare in AMPs and are mostly found near the N terminus (37–39). Aromatic residues have the unique property of being able to interact with the interfacial region of a membrane, thereby anchoring the peptide to the bilayer surface, and they are very common in viral fusion peptides

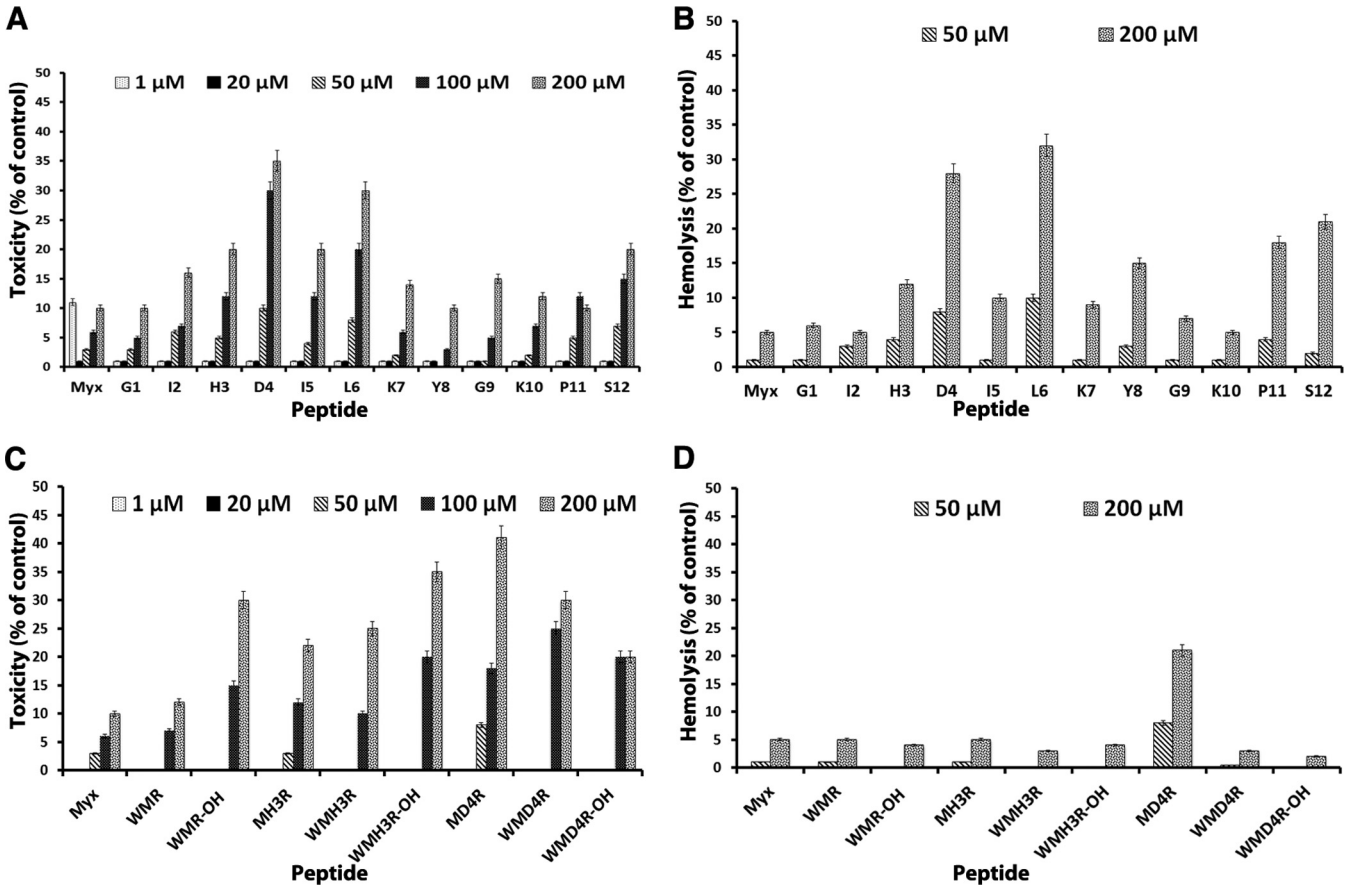

FIG 3 Toxicity of native myxinidin and alanine scanning peptides (A) and analogues (C), determined using the MTT assay. The viability of Vero cells in each well was presented as a percentage of the control cells. The hemolytic activity of peptides was monitored by measuring the absorbance of the supernatant at 540 nm in alanine scanning peptides (B) and analogues (D).

(40–42). Aromatic residue-containing peptides possess the unique ability to interact with the surface of bacterial cell membranes. Our data further support the key role played by aromatic residues in antibacterial activity.

The change of the charged residues Lys^7 and Lys^{10} (peptides K7 and K10) with alanine did not induce a complete loss of activity, but both peptides show reduced activity in all the Gram-negative bacteria compared to that with the native myxinidin. In particular, the substitution Lys→Ala reduces also the net charge of the peptide, and thus, it is conceivable that it reduces activity.

The modification of Gly^1, His^3, Ile^5, Gly^9, and Pro^{11} (peptides G1, H3, I5, G9, and P11, respectively) retained or increased antibacterial activity in all bacteria and especially against *S.* Typhimurium (Fig. 5A). Notably, the substitution of Gly^9 determines an increased activity against all Gram-negative bacteria.

The antimicrobial activity of the modified peptides demonstrated that the positions 2, 4, 6, 8, and 12 are fundamental for activity, especially in *P. aeruginosa* and *S.* Typhimurium; positions 1, 3, 5, and 11 are not essential for activity, since they all had the same or double the antimicrobial activity as that of native myxinidin. It is also interesting to note that peptides M4 and M6 show a higher activity also for the Gram-positive bacterium *S. aureus*.

We previously reported the results obtained from antibacterial experiments performed on myxinidin analogues. In particular, we reported increased activity for peptides MH3R (in which His^3 was substituted with Arg) and MD4R (in which Asp^4 was substituted with Arg). These data are in agreement with the alanine scanning results; His^3 is not essential for activity, and position 4 has to be occupied by a charged residue, with a preference for positively charged amino acids. We also previously reported that the analogue WMR (with an amidated C terminus) was very active against all bacteria, further supporting the key role played by aromatic residues located at the N terminus. We thus decided to synthetize two new sequences derived from MH3R and MD4R by adding a Trp at the N terminus to verify if the addition of the tryptophan to a single-residue mutant was enough to increase activity (Fig. 6). Our results show that this modification did not induce a significant enhancement in activity, with the sequence WMR still being the one with the highest activity (see Table S4 in the supplemental material); the simultaneous substitutions of residues present in positions 3, 4, and 11 with arginine and the addition of the tryptophan at the N terminus resulted in a significant increase in activity. We also synthetized the peptide WMR with the free C terminus, but we did not observe the same increase in activity (see Table S4).

Hemolytic activity. The hemolytic activities of the peptides against human erythrocytes were determined as a measure of peptide toxicity toward higher eukaryotic cells. Red blood cells were incubated with different peptide solutions and Triton X-100 as a positive control. Some peptides at 50 μM led to about 10% hemo-

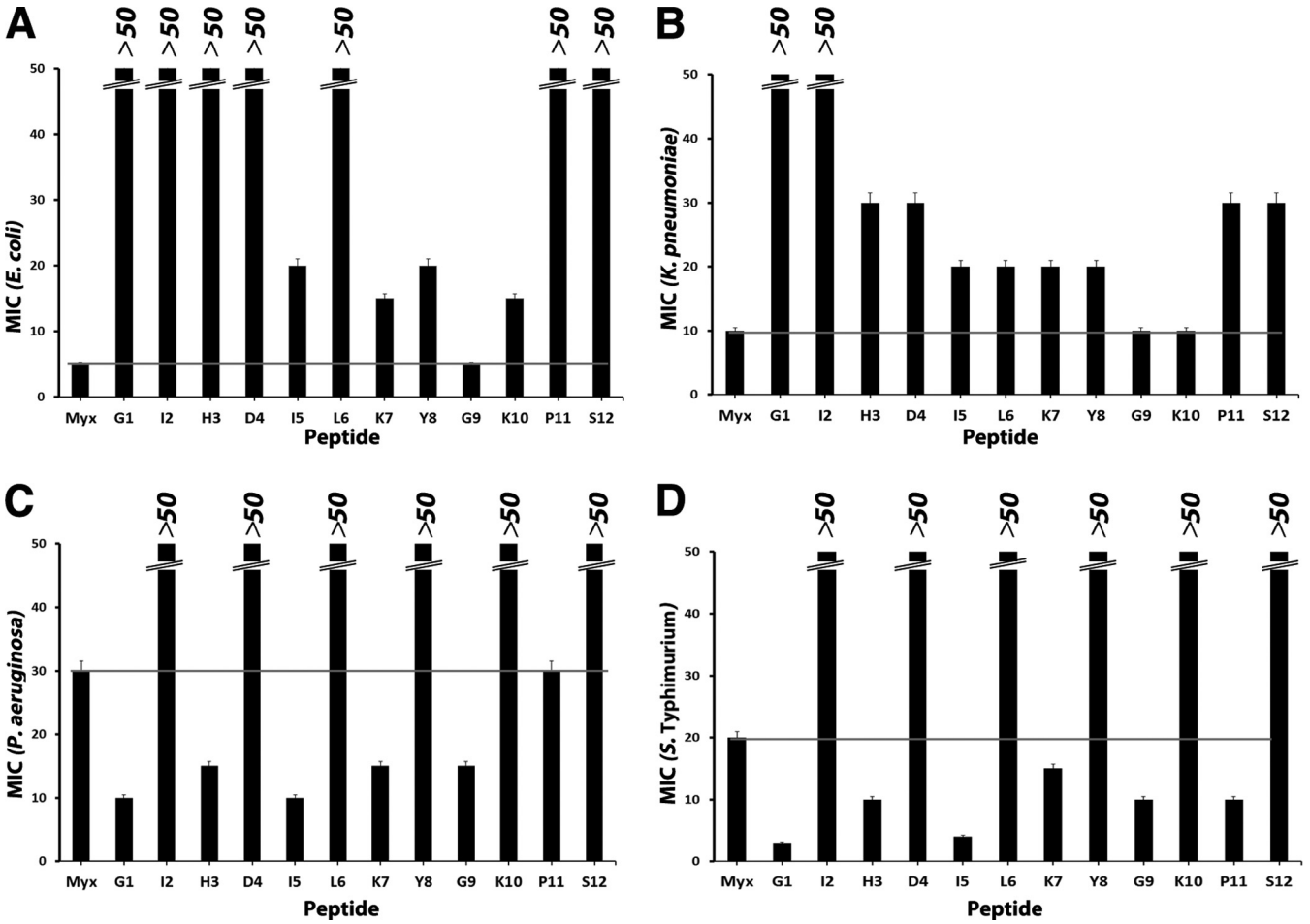

FIG 4 Myxinidin alanine scanning analogue MICs on different Gram-negative microbial strains.

lysis, but in general, negligible hemolytic activity was observed even at 100 μM and 200 μM peptide. (Fig. 3B and D). Minor hemolytic activity was observed at 100 μM and 200 μM concentrations. As a positive control, we used the peptide melittin, which is known to possess high hemolytic activity.

DISCUSSION

Mapping of the functional activity of each residue of myxinidin provides a solid basis for engineering a bacterium-specific antimicrobial.

The relatively short linear myxinidin peptide is unstructured in a water solution. Being cationic, it preferentially binds to the negatively charged membrane of bacteria over mammalian cells (43, 44). The interaction with lipids in the bilayer probably induces helix formation, as reported for other AMPs (37–39, 45, 46) and as demonstrated by the tendency to adopt a helical conformation in TFE, so that direct interaction with the lipid bilayer might also assist penetration. It is widely accepted that after reaching the microbial cytoplasmic membrane, AMPs initially interact with the negatively charged head groups of the external leaflet and then assume an amphipathic helical conformation that allows them to insert the hydrophobic face into the bilayer (37–39, 46, 47). The formation of the α-helical structure before membrane interaction may not be advantageous; the antimicrobial potency may be related to the inducibility of a helical conformation in a membrane-mimicking environment rather than to the intrinsic helical stability (37–39, 47). The initial electrostatic interaction and the following hydrophobic partition provide AMPs with the unique ability to be highly water soluble but also to be able to interact strongly with negatively charged phospholipid bilayers (37–39, 48).

A previous study (16) showed the ability of peptides to structure into a well-defined amphipathic α-helix and also that the type of cationic residues and the percentage of hydrophobic residues were key factors in determining their antibacterial and hemolytic activities. The modification of residues onto the polar face was performed to increase their net positive charge. In the present study, further details of the peptide structure were investigated using an alanine scanning mutagenesis. CD analyses revealed that the native peptide contains a significant degree of helical conformation in the presence of a solvent, which mimics the hydrophobic environment of the membrane bilayer (Fig. 1). High-resolution NMR in buffer indicated that the peptide is flexible and lacks ordered secondary structure elements. In contrast, in the presence of TFE, it assumes an ordered α-helical structure, which involves residues 2 to 9. Our data further support the view that after the initial ionic interaction with the head groups of the bilayer, the folding of the peptide into an α-helix induces the penetration of and is responsible for the antimicrobial activity. The analysis of the CD data clearly demonstrates that all the analogues do not

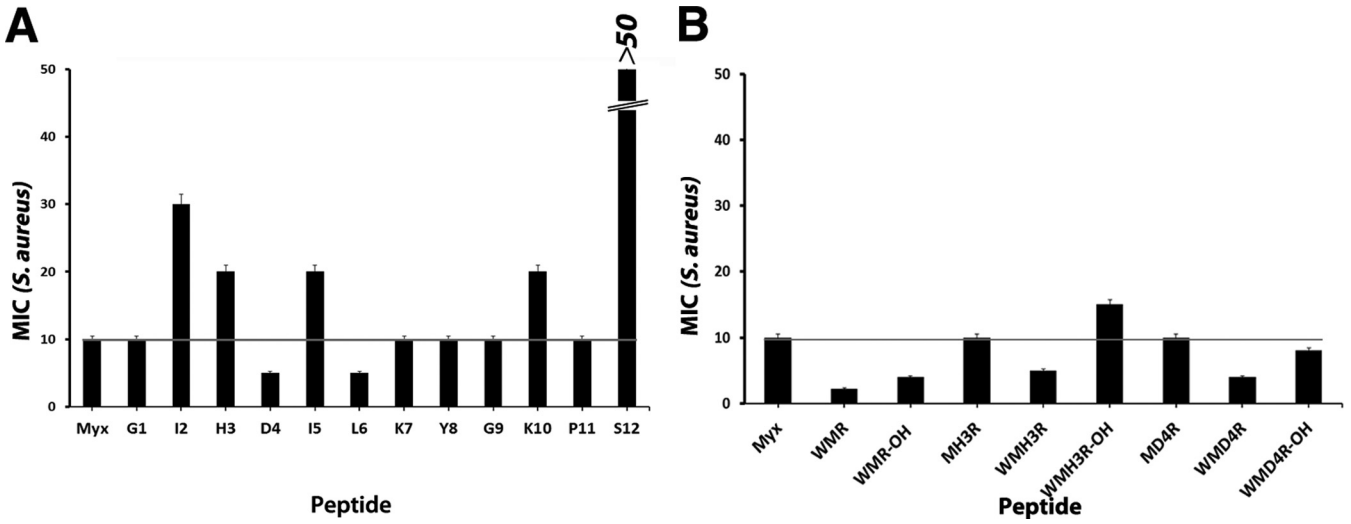

FIG 5 Myxinidin analogue MICs on *S. aureus* alanine scanning peptides (A) and analogues (B).

assume a defined conformation in buffer while they approach a helix-like conformation in membrane-mimicking environments. The conservation of the helical structure in TFE supports the key role played by the identity and character of the amino acids in the activity. In fact, our data can be placed in the context of studies on AMPs that clearly support the key role played by an appropriate balance of hydrophobicity, amphipathicity, and positive charge in α-helical peptides of this class for the enhancement of their ther-

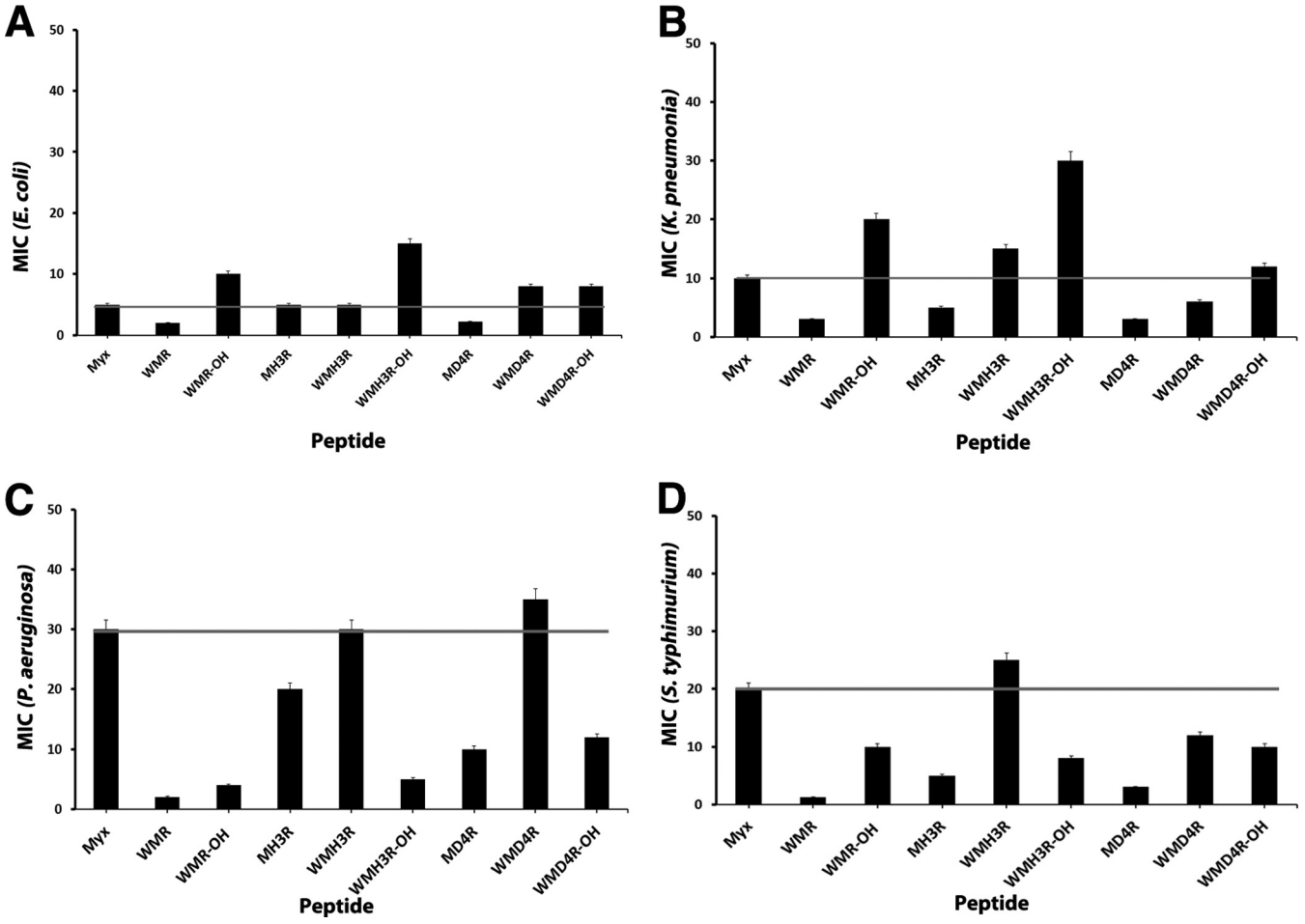

FIG 6 Myxinidin analogue MICs on different Gram-negative microbial strains.

apeutic potential. To design AMPs with higher potency, it is thus necessary to modulate charge, hydrophobicity, and amphipathicity, with a reduction in hydrophobicity determining a reduction in mammalian cell interactions while retaining the targeting of bacterial cell membranes, as long as the peptide has sufficient positive charge. Therefore, basic and hydrophobic residues play a key role in AMPs. Moreover, even though their target is the bacterial membrane, hemolytic activity and/or toxicity to mammalian cells represents a potential barrier to their use as systemic therapeutics. The goal of AMP development is to optimize biophysical parameters, minimize eukaryotic cell toxicity, and maximize antimicrobial activity. All the analogues showed minimal hemolytic activity and toxicity, which led us to further analyze their antimicrobial activities.

The analysis of the results obtained for the analogues reported in this study allows us to understand the structural determinants responsible for activity and represent a starting point for future quantitative structure-activity relationship (QSAR) studies.

Introducing a positive charge onto the nonpolar face of an amphipathic helix is an extreme way of disrupting amphipathicity, which nonetheless contributes both to the suppression of binding to membranes with little surface charge and to the enhancement of binding to negatively charged membranes (43). As a matter of fact, the substitution of Ser^{12} present on the hydrophobic face of myxinidin with alanine reduces significantly activity.

Gly_1 plays a key role; in fact, it is believed to improve the stability of peptides (49) and also is important for selectivity, as recently reported by Juretic et al. (37). Moreover, most AMPs start with a Gly. Interestingly, the substitution Gly→Ala in antibacterial assays against *P. aeruginosa* and *S.* Typhimurium results in an increase in activity while it results in a loss in activity in *E. coli* and *K. pneumoniae*.

Usually, the proline disrupts the α-helical structure by putting a kink in the polypeptide chain; in short amphipathic model peptides, the introduction of a proline in the middle of the nonpolar face determines a loss of approximately 50% of the helical content (50). The substitution of the proline with alanine induces a decrease in activity while maintaining the percentage of helical structures in TFE. The formation of the α-helical structure before engaging membrane interactions may not be helpful to the activity, while the antimicrobial potency may be related to the inducibility of a helical conformation in a membrane-mimicking environment. The common view on cationic AMPs is that after reaching the microbial cytoplasmic membrane, the peptide initially interacts with the negatively charged head groups of the external leaflet and then assumes an amphipathic helical conformation that allows them to insert the hydrophobic face into the bilayer (38, 39, 51).

The charge plays a key role in activity and, in particular, the substitution of the lysine residue on the polar face with alanine reduces activity. Sometimes, negatively charged residues are present on the polar face, but the reason why so many AMPs contain negatively charged residues remains unknown (37–39). Also, in our case, the substitution of the aspartic acid with alanine reduces activity, indicating that this position has to be occupied by a charged residue.

It is not easy to define the effects of the other substitutions, although we can say in general that amphipathicity plays a key role. Here, we report also the relative hydrophobic moment (μHrel), which should be 1 for a peptide that has the maximum possible amphipathicity. These parameters were calculated as previously reported (38, 39).

The results on alanine scanning analogues together with those obtained for previously reported analogues (16) helped in the design of novel sequences, which confirmed the highest activity of the WMR peptide (16). In particular, we obtained an increased activity for peptides MH3R (in which His_3 was substituted with Arg) and MD4R (in which Asp_4 was substituted with Arg) compared to the native sequence and in agreement with alanine scanning results; residues 3 and 4 are located on the charged face of the helix, and when occupied by a positively charged residue, they result in an increase of activity. Next, we probed the role of the tryptophan residue at the N terminus of the sequence, and we found that the simultaneous substitutions of residues present in positions 3, 4, and 11 with Arg and the addition of the Trp at the N terminus result in a significant increase in activity. However, the addition of the tryptophan to the single mutants did not determine the same increase of activity (peptides WMH3R and WMD4R). The analysis of the structural features of the analogues shows the key role played by the charge and the hydrophobicity in their activity.

The data obtained for *S. aureus* clearly show that activity correlates with net charge while requiring sufficient hydrophobicity and amphipathicity; in particular, the peptides with increased charge show a higher activity. Correspondingly, other studies identify charge as a critical parameter in the activity of helical AMPs (52); decreasing the net charge below +3 reduces potency, while increasing the net charge gradually increases activity (51, 53, 54). Bacterial surfaces contain many anionic components, including lipopolysaccharide (LPS) and anionic lipids of Gram-negative bacteria, as well as the teichoic and teichuronic acids of Gram-positive bacteria.

Of particular interest is the observation that the peptides can be grouped into those that are effective with *E. coli* and *K. pneumoniae* and those that are effective with *P. aeruginosa* and *S.* Typhimurium. It is thus noteworthy to find a correlation between the activity and the composition of the cytoplasmic membrane of the bacteria. The lipid composition in bacteria varies greatly, and, in addition, bacteria are able to modify their lipid composition in response to environmental conditions. Table S5 in the supplemental material reports the membrane compositions of the different bacteria that have been used in this study (32, 55).

The first difference is between Gram-negative and Gram-positive bacteria. The *S. aureus* lacks phosphatidylethanolamine (PE) in the cytoplasmic membrane, similar to most other Gram-positive bacteria, presenting instead mostly phospholipids with anionic head groups (phosphatidylglycerol [PG] or cardiolipin [CL]). As a matter of fact, peptide M4 and all those in Table S4 in the supplemental material present significant activity against *S. aureus*.

The analysis of the membrane composition pinpoints the fact that Gram-negative bacteria contain PE, PG, and CL, and a deeper analysis shows that *E. coli* and *K. pneumoniae* contain a higher percentage of PE than PG and CL, while *P. aeruginosa* and *S.* Typhimurium contain a lower percentage of PE than the sum of the negatively charged PG and CL. This result may correlate to the greater susceptibility to charged residues for these last two bacteria, as obtained from the analysis of the antibacterial data.

In contrast, the membrane of eukaryotic cells has a high percentage of zwitterionic lipids and a low content of negatively

charged lipids, which accounts for the low toxicity and hemolytic activities.

The ability to assume a helical conformation in a membrane-like environment is a key element for microbial inactivation, but several other factors seem to play a fundamental role, including (i) the presence of helix-stabilizing (Leu, Ala, and Lys) or -destabilizing (Pro) residues, (ii) the effects of substitutions on the helix dipole, (iii) the disruption of the nonpolar face, and (iv) the number of positive charges.

By virtue of the propensity to bind preferentially to anionic bacterial membranes, AMPs have broad-spectrum antibacterial activities against Gram-negative and Gram-positive bacteria but limited toxicity on mammalian membranes and might be useful as broad-spectrum antibiotics. In summary, the experiments described in this study have highlighted the possibility of widening the original spectrum of action of myxinidin by making suitable changes in the peptide primary structure. Our findings show that myxinidin, having a simple composition, a broad spectrum of antimicrobial activity, and no hemolytic activity, is a promising candidate for the design of novel AMPs, with improved antimicrobial activity and very low hemolytic effect.

ACKNOWLEDGMENTS

We thank Leopoldo Zona and Luca De Luca for excellent technical assistance.

Financial support was provided by MIUR-PON01_02388 "Verso la medicina personalizzata: nuovi sistemi molecolari per la diagnosi e la terapia di patologie oncologiche ad alto impatto sociale" Salute dell'uomo e Biotecnologies.

We declare no conflicts of interest.

REFERENCES

1. **Livermore DM.** 2009. Has the era of untreatable infections arrived? J. Antimicrob. Chemother. **64**(Suppl 1):i29–i36. http://dx.doi.org/10.1093/jac/dkp255.
2. **Hawkey PM.** 2008. The growing burden of antimicrobial resistance. J. Antimicrob. Chemother. **62**(Suppl 1):i1–i9. http://dx.doi.org/10.1093/jac/dkn241.
3. **Choi KY, Chow LN, Mookherjee N.** 2012. Cationic host defence peptides: multifaceted role in immune modulation and inflammation. J. Innate Immun. **4:**361–370. http://dx.doi.org/10.1159/000336630.
4. **Bowdish DM, Davidson DJ, Hancock RE.** 2005. A re-evaluation of the role of host defence peptides in mammalian immunity. Curr. Protein Pept. Sci. **6:**35–51. http://dx.doi.org/10.2174/1389203053027494.
5. **Zhao X, Wu H, Lu H, Li G, Huang Q.** 2013. LAMP: a database linking antimicrobial peptides. PLoS One **8:**e66557. http://dx.doi.org/10.1371/journal.pone.0066557.
6. **Jenssen H, Hamill P, Hancock RE.** 2006. Peptide antimicrobial agents. Clin. Microbiol. Rev. **19:**491–511. http://dx.doi.org/10.1128/CMR.00056-05.
7. **Wiesner J, Vilcinskas A.** 2010. Antimicrobial peptides: the ancient arm of the human immune system. Virulence **1:**440–464. http://dx.doi.org/10.4161/viru.1.5.12983.
8. **Zasloff M.** 2002. Antimicrobial peptides of multicellular organisms. Nature **415:**389–395. http://dx.doi.org/10.1038/415389a.
9. **Wang Z, Wang G.** 2004. APD: the antimicrobial peptide database. Nucleic Acids Res. **32:**D590–D592. http://dx.doi.org/10.1093/nar/gkh025.
10. **Seshadri Sundararajan V, Gabere MN, Pretorius A, Adam S, Christoffels A, Lehväslaiho M, Archer JA, Bajic VB.** 2012. DAMPD: a manually curated antimicrobial peptide database. Nucleic Acids Res. **40:**D1108–D1112. http://dx.doi.org/10.1093/nar/gkr1063.
11. **Ellis AE.** 2001. Innate host defense mechanisms of fish against viruses and bacteria. Dev. Comp. Immunol. **25:**827–839. http://dx.doi.org/10.1016/S0145-305X(01)00038-6.
12. **Masso-Silva J, Diamond G.** 2014. Antimicrobial peptides from fish. Pharmaceuticals (Basel) **7:**265–310. http://dx.doi.org/10.3390/ph7030265.
13. **Rakers S, Niklasson L, Steinhagen D, Kruse C, Schauber J, Sundell K, Paus R.** 2013. Antimicrobial peptides (AMPs) from fish epidermis: perspectives for investigative dermatology. J. Invest. Dermatol. **133:**1140–1149. http://dx.doi.org/10.1038/jid.2012.503.
14. **Subramanian S, Ross NW, MacKinnon SL.** 2009. Myxinidin, a novel antimicrobial peptide from the epidermal mucus of hagfish, *Myxine glutinosa* L. Mar. Biotechnol. (NY) **11:**748–757. http://dx.doi.org/10.1007/s10126-009-9189-y.
15. **Subramanian S, Ross NW, Mackinnon SL.** 2008. Comparison of the biochemical composition of normal epidermal mucus and extruded slime of hagfish (*Myxine glutinosa* L.). Fish Shellfish Immunol. **25:**625–632. http://dx.doi.org/10.1016/j.fsi.2008.08.012.
16. **Cantisani M, Leone M, Mignogna E, Kampanaraki K, Falanga A, Morelli G, Galdiero M, Galdiero S.** 2013. Structure-activity relations of myxinidin, an antibacterial peptide derived from the epidermal mucus of hagfish. Antimicrob. Agents Chemother. **57:**5665–5673. http://dx.doi.org/10.1128/AAC.01341-13.
17. **Cunningham BC, Wells JA.** 1989. High-resolution epitope mapping of hGH-receptor interactions by alanine-scanning mutagenesis. Science **244:**1081–1085. http://dx.doi.org/10.1126/science.2471267.
18. **Galdiero S, Capasso D, Vitiello M, D'Isanto M, Pedone C, Galdiero M.** 2003. Role of surface-exposed loops of *Haemophilus influenzae* protein P2 in the mitogen-activated protein kinase cascade. Infect. Immun. **71:**2798–2809. http://dx.doi.org/10.1128/IAI.71.5.2798-2809.2003.
19. **Chakrabartty A, Kortemme T, Baldwin RL.** 1994. Helix propensities of the amino acids measured in alanine-based peptides without helix-stabilizing side-chain interactions. Protein Sci. **3:**843–852.
20. **Galdiero S, Falanga A, Vitiello M, D'Isanto M, Cantisani M, Kampanaraki A, Benedetti E, Browne H, Galdiero M.** 2008. Peptides containing membrane-interacting motifs inhibit herpes simplex virus type 1 infectivity. Peptides **29:**1461–1471. http://dx.doi.org/10.1016/j.peptides.2008.04.022.
21. **Dalvit C.** 1998. Efficient multiple-solvent suppression for the study of the interactions of organic solvents with biomolecules. J. Biomol. NMR **11:**437–444. http://dx.doi.org/10.1023/A:1008272928075.
22. **Wüthrich K.** 1986. NMR of proteins and nucleic acids. John Wiley & Sons, New York, NY.
23. **Griesinger C, Otting G, Wüthrich K, Ernst RR.** 1988. Clean TOCSY for proton spin system identification in macromolecules. J. Am. Chem. Soc. **110:**7870–7872. http://dx.doi.org/10.1021/ja00231a044.
24. **Kumar A, Ernst RR, Wüthrich K.** 1980. A two-dimensional nuclear Overhauser enhancement (2D NOE) experiment for the elucidation of complete proton-proton cross-relaxation networks in biological macromolecules. Biochem. Biophys. Res. Commun. **95:**1–6. http://dx.doi.org/10.1016/0006-291X(80)90695-6.
25. **Piantini U, Sorensen OW, Ernst RR.** 1982. Multiple quantum filters for elucidating NMR coupling networks. J. Am. Chem. Soc. **104:**6800–6801. http://dx.doi.org/10.1021/ja00388a062.
26. **Bartels C, Xia TH, Billeter M, Güntert P, Wüthrich K.** 1995. The program XEASY for computer-supported NMR spectral analysis of biological macromolecules. J. Biomol. NMR **6:**1–10. http://dx.doi.org/10.1007/BF00417486.
27. **Herrmann T, Güntert P, Wüthrich K.** 2002. Protein NMR structure determination with automated NOE assignment using the new software CANDID and the torsion angle dynamics algorithm DYANA. J. Mol. Biol. **319:**209–227. http://dx.doi.org/10.1016/S0022-2836(02)00241-3.
28. **Koradi R, Billeter M, Wüthrich K.** 1996. MOLMOL: a program for display and analysis of macromolecular structures. J. Mol. Graph. **14:**51–55, 29–32.
29. **Doreleijers JF, Sousa da Silva AW, Krieger E, Nabuurs SB, Spronk CA, Stevens TJ, Vranken WF, Vriend G, Vuister GW.** 2012. CING: an integrated residue-based structure validation program suite. J. Biomol. NMR **54:**267–283. http://dx.doi.org/10.1007/s10858-012-9669-7.
30. **Doreleijers JF, Vranken WF, Schulte C, Markley JL, Ulrich EL, Vriend G, Vuister GW.** 2012. NRG-CING: integrated validation reports of remediated experimental biomolecular NMR data and coordinates in wwPDB. Nucleic Acids Res. **40:**D519–D524. http://dx.doi.org/10.1093/nar/gkr1134.
31. **Mosmann T.** 1983. Rapid colorimetric assay for cellular growth and survival: application to proliferation and cytotoxicity assays. J. Immunol. Methods **65:**55–63. http://dx.doi.org/10.1016/0022-1759(83)90303-4.
32. **Ames GF.** 1968. Lipids of *Salmonella* Typhimurium and *Escherichia coli*: structure and metabolism. J. Bacteriol. **95:**833–843.
33. **Buck M.** 1998. Trifluoroethanol and colleagues: cosolvents come of age. Recent studies with peptides and proteins. Q. Rev. Biophys. **31:**297–355.
34. **Wishart DS, Sykes BD, Richards FM.** 1991. Relationship between nuclear

magnetic resonance chemical shift and protein secondary structure. J. Mol. Biol. **222:**311–333. http://dx.doi.org/10.1016/0022-2836(91)90214-Q.

35. **Jiang Z, Vasil AI, Gera L, Vasil ML, Hodges RS.** 2011. Rational design of α-helical antimicrobial peptides to target Gram-negative pathogens, *Acinetobacter baumannii* and *Pseudomonas aeruginosa*: utilization of charge, 'specificity determinants,' total hydrophobicity, hydrophobe type and location as design parameters to improve the therapeutic ratio. Chem. Biol. Drug Des. **77:**225–240. http://dx.doi.org/10.1111/j.1747-0285.2011.01086.x.
36. **Hawrani A, Howe RA, Walsh TR, Dempsey CE.** 2008. Origin of low mammalian cell toxicity in a class of highly active antimicrobial amphipathic helical peptides. J. Biol. Chem. **283:**18636–18645. http://dx.doi.org/10.1074/jbc.M709154200.
37. **Juretić D, Vukičević D, Ilić N, Antcheva N, Tossi A.** 2009. Computational design of highly selective antimicrobial peptides. J. Chem. Infect. Model. **49:**2873–2882. http://dx.doi.org/10.1021/ci900327a.
38. **Giangaspero A, Sandri L, Tossi A.** 2001. Amphipathic alpha-helical antimicrobial peptides. Eur. J. Biochem. **268:**5589–5600. http://dx.doi.org/10.1046/j.1432-1033.2001.02494.x.
39. **Tossi A, Sandri L, Giangaspero A.** 2000. Amphipathic, alpha-helical antimicrobial peptides. Biopolymers **55:**4–30. http://dx.doi.org/10.1002/1097-0282(2000)55:1<4::AID-BIP30>3.0.CO;2-M.
40. **Galdiero S, Russo L, Falanga A, Cantisani M, Vitiello M, Fattorusso R, Malgieri G, Galdiero M, Isernia C.** 2012. Structure and orientation of the gH625–644 membrane interacting region of herpes simplex virus type 1 in a membrane mimetic system. Biochemistry **51:**3121–3128. http://dx.doi.org/10.1021/bi201589m.
41. **Falanga A, Tarallo R, Vitiello G, Vitiello M, Perillo E, Cantisani M, D'Errico G, Galdiero M, Galdiero S.** 2012. Biophysical characterization and membrane interaction of the two fusion loops of glycoprotein B from herpes simplex type I virus. PLoS One **7:**e32186. http://dx.doi.org/10.1371/journal.pone.0032186.
42. **Falanga A, Cantisani M, Pedone C, Galdiero S.** 2009. Membrane fusion and fission: enveloped viruses. Protein Pept. Lett. **16:**751–759. http://dx.doi.org/10.2174/092986609788681760.
43. **Dempsey CE, Hawrani A, Howe RA, Walsh TR.** 2010. Amphipathic antimicrobial peptides—from biophysics to therapeutics? Protein Pept. Lett. **17:**1334–1344. http://dx.doi.org/10.2174/0929866511009011334.
44. **Matsuzaki K.** 2009. Control of cell selectivity of antimicrobial peptides. Biochim. Biophys. Acta **1788:**1687–1692. http://dx.doi.org/10.1016/j.bbamem.2008.09.013.
45. **Bhargava K, Feix JB.** 2004. Membrane binding, structure, and localization of cecropin-mellitin hybrid peptides: a site-directed spin-labeling study. Biophys. J. **86:**329–336. http://dx.doi.org/10.1016/S0006-3495(04)74108-9.
46. **Turner J, Cho Y, Dinh NN, Waring AJ, Lehrer RI.** 1998. Activities of LL-37, a cathelin-associated antimicrobial peptide of human neutrophils. Antimicrob. Agents Chemother. **42:**2206–2214.
47. **Ladokhin AS, White SH.** 1999. Folding of amphipathic α-helices on membranes: energetics of helix formation by melittin. J. Mol. Biol. **285:**1363–1369. http://dx.doi.org/10.1006/jmbi.1998.2346.
48. **Matsuzaki K, Nakamura A, Murase O, Sugishita K, Fujii N, Miyajima K.** 1997. Modulation of magainin 2-lipid bilayer interactions by peptide charge. Biochemistry **36:**2104–2111. http://dx.doi.org/10.1021/bi961870p.
49. **Ma QQ, Shan AS, Dong N, Gu Y, Sun WY, Hu WN, Feng XJ.** 2011. Cell selectivity and interaction with model membranes of Val/Arg-rich peptides. J. Pept. Sci. **17:**520–526. http://dx.doi.org/10.1002/psc.1360.
50. **Wilman RH, Jiye S, Deane MC.** 2014. Helix kinks are equally prevalent in soluble and membrane proteins. Proteins Struct. Funct. Bioinform., in press. http://dx.doi.org/10.1002/prot.24550.
51. **Scudiero O, Galdiero S, Cantisani M, Di Noto R, Vitiello M, Galdiero M, Naclerio G, Cassiman JJ, Pedone C, Castaldo G.** 2010. Novel synthetic, salt-resistant analogs of human beta-defensins 1 and 3 endowed with enhanced antimicrobial activity. Antimicrob. Agents Chemother. **54:**2312–2322. http://dx.doi.org/10.1128/AAC.01550-09.
52. **Pasupuleti M, Walse B, Svensson B, Malmsten M, Schmidtchen A.** 2008. Rational design of antimicrobial C3a analogues with enhanced effects against staphylococci using an integrated structure and function-based approach. Biochemistry **47:**9057–9070. http://dx.doi.org/10.1021/bi800991e.
53. **Scudiero O, Galdiero S, Nigro E, Del Vecchio L, Di Noto R, Cantisani M, Colavita I, Galdiero M, Cassiman JJ, Daniele A, Pedone C, Salvatore F.** 2013. Chimeric beta-defensin analogs, including the novel 3NI analog, display salt-resistant antimicrobial activity and lack toxicity in human epithelial cell lines. Antimicrob. Agents Chemother. **57:**1701–1708. http://dx.doi.org/10.1128/AAC.00934-12.
54. **Harder J.** 2001. Isolation and characterization of human beta-defensin3, a novel human inducible peptide antibiotic. J. Biol. Chem. **276:**5707–5713. http://dx.doi.org/10.1074/jbc.M008557200.
55. **Epand RF, Pollard JE, Wright JO, Savage PB, Epand RM.** 2010. Depolarization, bacterial membrane composition, and the antimicrobial action of ceragenins. Antimicrob. Agents Chemother. **54:**3708–3713. http://dx.doi.org/10.1128/AAC.00380-10.